Bonding Patterns in Transition Metal Clusters

A. CEULEMANS

Department of Chemistry, University of Leuven, Celestijnenlaan 200F, 3030 Leuven, Belgium

and P. W. FOWLER

Department of Theoretical Chemistry, University Chemical Laboratory, Lensfield Road, Cambridge CB2 1EW, U.K.

Received February 25, 1985

Abstract

Bonding patterns and electron counts of high-symmetry transition metal cluster compounds are discussed using a simplified Tensor Surface Harmonic (TSH) treatment. An n-vertex metal cluster has 9n valence atomic orbitals. From this set orbitals concerned in metal–ligand bonding are eliminated to yield the effective valence orbitals available to cluster bonding. Applying TSH theory to this smaller set gives a clear classification of the cluster MOs and their bonding/antibonding characteristics. Orbital mixing allowed by point group symmetry gives a final, qualitative cluster MO diagram. Results for triangular, tetrahedral and octahedral clusters are compared with other models.

Introduction

Electron counting schemes for boranes and hydrocarbon clusters are to a certain extent transferable to isostructural clusters of transition-metals [1–3]. This is an interesting observation since it suggests that an understanding of skeletal bonding in a wide range of compounds can be based on a common approach, taking into account only the geometry and connectivity of the polyhedral network. At first sight it is surprising that the electronic structure of a cage of main-group atoms which have four valence orbitals should be analogous to the structure of a cage of transition-metal atoms which have no less than nine valence orbitals (in the case of a first-row transition-metal these are 3d, 4s, 4p).

The short answer to this problem is that interactions between the ligand envelope and the metal skeleton drastically reduce the number of metal orbitals that are effectively available for cluster bonding, thus re-establishing a link with main-group element valence structure. Recently Stone explained in general terms how these interactions may be visualized [4, 5]. His description is based on the Tensor Surface Harmonic (TSH) theory [6]. In this paper we present an equivalent description of the metal–metal bonding in clusters, which also makes use of the TSH formalism, but grafts it onto a more typically chemical way of thinking. Our approach is illustrated in a survey of several well-established metal clusters of D_{3h}, T_d and O_h symmetries.

The TSH Treatment of Metal Clusters

The idealized site symmetry of a metal atom in a globular cluster is $C_{\infty v}$. For a site on the z-axis the basis orbital set is seen to consist of three σ-type orbitals (s, p_z, d_{z^2}), four π-type orbitals (p_x, p_y, d_{xz}, d_{yz}), and two δ-type orbitals (d_{xy}, $d_{x^2-y^2}$). As has been shown by Stone these fragment orbitals can be recombined into molecular orbitals, which derive from parent tensor spherical harmonics [4, 5]. The resulting orbital combinations are labeled L_s^{σ}, L_p^{σ}, L_d^{σ}, L_p^{π}, L_d^{π}, L_d^{δ}, $\bar{L}_p^{\pi}$, $\bar{L}_d^{\pi}$, $\bar{L}_d^{\delta}$ where the indices refer to the type of fragment orbital, L denotes the parent axial surface harmonic and $\bar{L}$ symbolizes its polar counterpart. In this way one generates an embarassingly large collection of orbitals [5]. Extensive interactions between orbitals of the same point-group symmetry will certainly occur, yielding linear combinations of mixed parentage. As an example equisymmetric $\bar{L}_p^{\pi}$ and $\bar{L}_d^{\pi}$ orbital pairs will repel each other to form inward- (*endo*) and outward- (*exo*) pointing combinations. Since both levels are metal–metal antibonding the *endo* combination can be expected to be strongly cluster antibonding, while the *exo* combination will probably not affect the cluster bonding, but can be assumed to accept ligand electron pairs.

By pursuing this analysis one is able to filter out strongly metal–metal antibonding levels, leaving an assorted residue of non-bonding, metal–metal bonding and metal–ligand bonding levels. As it turned out, there is a one-to-one correspondence between the antibonding metal functions, which can be

0020-1693/85/$3.30

identified in this way, and the cluster antibonding orbitals in isostructural boranes. Electron counting analogies between electron-deficient boranes and electron-rich metal carbonyl clusters were thus ascribed to a common set of inaccessible orbitals, which must remain vacant in both types of clusters [4, 5]. These conclusions had been reached in the work of Mingos [7] and Lauher [8] based on specific Extended Hückel Calculations. As an example: in an octahedral metal cluster such as $Co_6(CO)_{16}$, with 43 electron pairs for 54 metal valence orbitals, 11 valence orbitals remain unoccupied. Exactly the same number of valence orbitals is vacant in the octahedral closo-borane $B_6H_6^{2-}$, with only 13 electron pairs for 24 valence orbitals.

While this analysis provides a general rationalization of the transferability of electron counting schemes, several deficiencies must be noted. First, as indicated by Woolley, electron pairs of the ligands are formally identified as metal pairs since they are used to fill up valence orbitals of the metal [9]. Second, only the inaccessible orbitals are well characterized. Important questions, such as the nature of the highest occupied cluster orbital, are not addressed. Third, the clarity of the TSH orbital classification in the initial stage of the treatment is greatly obscured by the subsequent extensive orbital mixing under the finite point-group symmetry.

Apparently the full power of the Stone approach may be utilized in a more economic way if irrelevant levels are removed before the TSH formalism enters the field, rather than afterwards. This can be done by considering metal–ligand interactions before cluster formation. Our method thus involves the following steps:

(i) First consider the isolated fragments of a metal ion and its surrounding ligands. Metal valence hybrids directed towards the σ-donating orbitals of the ligand will be involved in metal–ligand bonding and are not available for cluster bonding. As usual the ligand electron pair enters a ligand localized bonding combination, while the empty antibonding combination is mainly metal-localized. As a result, for each ligand electron pair a metal valence orbital is made inaccessible. This explains why ligand electrons may be formally allocated to metal valence orbitals.

(ii) The remaining metal orbitals will be referred to as the effecitve valence orbitals of the fragment. They include the fragment frontier orbitals, which form the building blocks of the isolobal approach [10–12], but also the non-bonding d-type orbitals. All these hybrids may be characterized by σ, π or δ labels. For non-conical fragments π or δ orbitals do not necessarily occur in pairs [13].

(iii) Next the TSH method is applied to the reduced set of hybrids which are effectively available for cluster bonding. Resulting levels will be characterized by L^{σ}, L^{π}, L^{δ}, $\bar{L}^{\pi}$, $\bar{L}^{\delta}$ labels. Where needed subscripts designating particular hybrids may be added.

(iv) Finally, finite point group symmetry is introduced [14] and interactions between equisymmetric orbitals are taken into account [15].

(v) Ligands in bridging positions require special attention. If these ligands in their ususal oxidation states can donate an electron pair to each surrounding metal, such pairs can of course be included in the first step of the method. If however coordination of the bridging ligands takes place *via* delocalized multicentre bonds, these interactions can only be introduced after delocalized cluster orbitals have been formed, *i.e.* in the fourth step.

By this series of steps we have identified the atomic orbitals relevant to cluster bonding, used TSH theory to construct cluster MOs and assign bonding/antibonding character to them and then considered how symmetry-allowed mixing modifies the bonding pattern. Of course this approach has much in common with Stone's all-orbital treatment, but it yields a simple solution to the problem of separating metal–ligand and metal–metal interactions, that is in close contact with current chemical thinking [16] and leads to a more transparent use of the elegant TSH formalism. The method will now be applied to a number of highly symmetric clusters, which share the remarkable property that their bonding pattern may be derived almost entirely from qualitative considerations, without numerical calculation.

Applications

(a) Triangular Clusters with four Effective Valence Orbitals

As a simple example consider the $Re_3Cl_{12}^{3-}$ anion (**1**) which forms an equilateral triangle with three μ_2-bridging chloride ligands [17]. Clearly a μ_2-Cl^- ligand may act as a 2 pair σ-donor, so that each Re-atom will be surrounded by five electron pairs, in a square pyramidal configuration (**2**). Five valence hybrids of sp^3d-type will be used up in Re–Cl bonds, leaving only four effective valence orbitals: one σ, two π and only one δ. In the cartesian frame of **2**, the latter orbital corresponds to d_{xy}. In more general terms it may be described as a $\delta(a_2)$-type

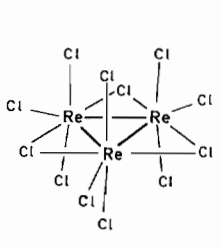

1

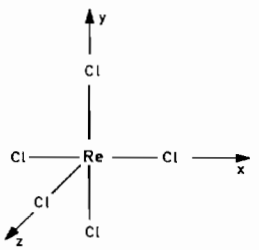

2

orbital, where the a_2 index refers to its symmetry representation in the actual C_{2v} site symmetry of the fragment. Straightforward application of the TSH method on this limited basis set yields the cluster molecular orbitals shown in Table I. In the final step orbitals with the same D_{3h} symmetry are allowed to interact. In the present case this does not affect the bonding pattern: $P^{\pi}(e')$ and $D^{\delta}(e'')$ become more bonding, whereas the $P^{\sigma}(e')$ and $\bar{P}^{\pi}(e'')$ levels become more antibonding. Hence one expects six cluster bonding levels, which will be occupied by the six electron pairs of the Re_3^{9+} cluster. In all probability the LUMO will be a $\bar{D}^{\delta}(a_1'')$ orbital. These conclusions agree well with recent calculations [18].

TABLE I. TSH Description of Bonding and Antibonding MO's in a Triangular Cluster, Based on Fragment Orbitals of σ, π and $\delta(a_2)$ Type. The Labels in Brackets Refer to D_{3h} Representations.

	σ	π^2	$\delta(a_2)$
bonding	$S^{\sigma}(a_1')$	$P^{\pi}(a_2'', e')$	$D^{\delta}(e'')$
anti-bonding	$P^{\sigma}(e')$	$\bar{P}^{\pi}(a_2', e'')$	$\bar{D}^{\delta}(a_1'')$

(b) Tetrahedral Clusters with Five Effective Valence Orbitals

A paradigmatic case of a tetrahedral cluster with four effective valence orbitals is the stable diamagnetic cubane-type cluster $Fe_4(NO)_4(\mu_3\text{-}S)_4$ (**3**) with approximate T_d-symmetry. According to current bonding models this cluster is electron-precise [19, 20], a conclusion which will now be confronted with a TSH approach. Following Dahl, nitrosyl will be treated as a two electron donor in its cationic state.

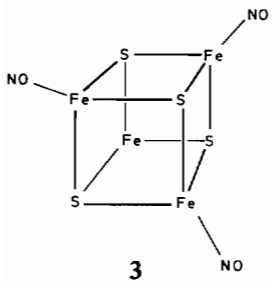

3

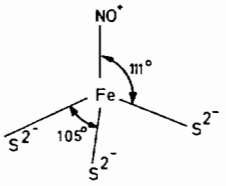

4

The sulfide ion may act as a three pair donor, pointing one electron pair to each Fe atom in a tetrahedral face. Consequently the isolated fragment exhibits approximate tetrahedral coordination (**4**). Metal–ligand interactions therefore consume four sp^3 (or sd^3) valence hybrids, thus reducing the effective valence shell of the Fe atoms to only five orbitals, with one σ, two π and two δ species. The results of a TSH treatment of the valence shell are displayed in Table II. Orbital interactions in T_d symmetry between the three t_2-orbitals will produce the usual antibonding ($\approx P^{\sigma}(t_2)$), non-bonding ($\approx D^{\delta}(t_2)$) and bonding ($\approx P^{\pi}(t_2)$) triad. Similarly the doublets of e and t_1-type orbitals recombine to one bonding and one antibonding combination. In any case the orbitals with approximate $P^{\sigma}(t_2)$ and $\bar{P}^{\pi}(t_1)$ signature will be inaccessible. The 14 metal electron pairs of an Fe_4^{4+} core will occupy all 14 remaining combinations, giving rise to a stable, closed-shell ground state. The analysis furthermore suggests a $\bar{P}^{\pi}(t_1)$ LUMO and an e-type HOMO of mixed $D^{\delta}\bar{D}^{\delta}$ and $D^{\pi}\bar{D}^{\pi}$ character. The assignment of the LUMO is in agreement with a Fenske-Hall calculation and also seems to be confirmed by the observed Jahn-Teller distortion in the singly reduced species $Fe_4(NO)_4(\mu_3\text{-}S)_4^-$ [19].

TABLE II. TSH Description of Molecular Orbitals in a Tetrahedral Cluster, Based on Fragment Orbitals of σ, π and δ Type. Labels in Brackets Refer to T_d Representations.

	σ	π^2	δ^2
bonding	$S^{\sigma}(a_1)$	$P^{\pi}(t_2)$	$D^{\delta}(t_2)$
nonbonding		$D^{\pi}\bar{D}^{\pi}(e)$	$D^{\delta}\bar{D}^{\delta}(e)$
antibonding	$P^{\sigma}(t_2)$	$\bar{P}^{\pi}(t_1)$	$\bar{D}^{\delta}(t_1)$

Essentially the same electronic structure prevails in the stable neutral cluster $Fe_4Cp_4(\mu_3\text{-}CO)_4$ [20]. At first sight the fragment coordination seems to be different: the *exo*-ligand NO^+ is replaced by a three pair donor, $\eta^5\text{-}C_5H_5^-$, whereas the three-pair bridging S^{2-} is replaced by a single-pair bridging CO (**5**). Clearly CO as a bridging ligand lacks electron

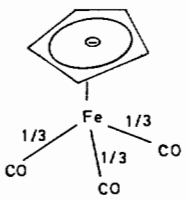

5

pairs to form localized σ-bonds with the three Fe atoms of a tetrahedral face, so that on the fragment level only three valence orbitals can be removed, accounting for penta-hapto coordination of the cyclopentadienyl anion. Six effective valence orbitals are left over, forming a $\sigma^2\pi^2\delta^2$ effective valence shell. Application of the TSH construction method thus leads to a doubling of the σ-type cluster orbitals, $a_1 + t_2$, as compared to the results for a $\sigma\pi^2\delta^2$ shell

in Table II. However the four lone pair orbitals of the CO bridges also yield the same symmetry representations $a_1 + t_2$, thus formally matching one set of

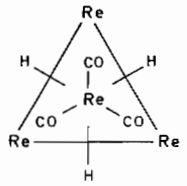

6

σ-type valence levels. In consequence delocalized bonding between the metals and the bridging ligands will remove one more σ-orbital per metal, so that the metal core in $Fe_4Cp_4(\mu_3\text{-}CO)_4$ again has only five effective valence orbitals, to be filled with fourteen electron pairs, exactly as in $Fe(NO)_4(\mu_3\text{-}S)_4$. Eight of these pairs of $t_1 + t_2 + e$ symmetry will receive an extra stabilization through interaction with the π-acceptor levels of CO.

As a final example we review the bonding pattern in the stable $Re_4(CO)_{12}H_4$ compound, which has three edge-eclipsed CO ligands per rhenium atom and face-bridging hydrides [21, 22]. The μ_3-H ligand in the hydridic form can be conceived as a one pair donor, exactly as the μ_3-CO ligand in $Fe_4Cp_4(\mu_3\text{-}CO)_4$. Similarly the three terminal CO ligands are equivalent to $\eta^5\text{-}C_5H_5^-$. Hence the total bonding pattern will be transferable, except that the Re_4^{4+} unit has four electrons less than Fe_4^{4+} and therefore the stable Re_4^{4+} configuration will be reached by depopulating the e-type HOMO of Fe_4^{4+}. The stability of the electron-deficient system thus confirms the assignment of the HOMO in the electron-rich analogue. For a more detailed account of the electronic structure of $M_4(CO)_{12}H_n$ and $M_4Cp_4H_n$ complexes the reader is referred to the work by Hoffmann *et al.* [23].

(c) Tetrahedral Clusters with Three Effective Valence Orbitals

In a cluster such as $Co_4Cp_4(\mu_3\text{-}S)_4$ (7), which is isostructural to $Fe_4Cp_4(\mu_3\text{-}CO)_4$, each cobalt atom is surrounded by six ligand electron pairs (8) as both Cp^- and S^{2-} are 3-lobe, 3 pair donors [24]. Metal–ligand interactions now require up to six valence orbitals, which will resemble the six well-known sp^3d^2 octahedral valence hybrids. Therefore only three valence orbitals, the familiar "t_{2g}" set, will be effectively available for cluster bonding. In an idealized trigonal site symmetry these orbitals transform as $a_1 + e$. The symmetry adapted combinations are:

$$a_1(t_{2g}) = d_{z^2}$$

$$e_a(t_{2g}) = \frac{1}{\sqrt{3}}(d_{xz} + \sqrt{2}d_{x^2-y^2})$$

$$e_b(t_{2g}) = \frac{1}{\sqrt{3}}(d_{yz} - \sqrt{2}d_{xy}) \qquad (1)$$

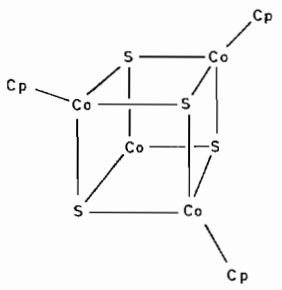

7

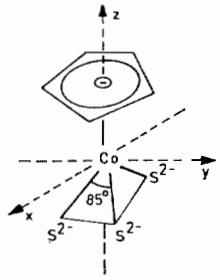

8

where a and b are C_s^{xz}-subrepresentations and x, y, z refer to the cartesian frame in 8. The $a_1(t_{2g})$ orbital is of the σ-type; the $e(t_{2g})$ orbitals are mixtures of π and δ in a 1:2 ratio, the trigonal site symmetry being unable to distinguish both labels.

From a qualitative point of view it is therefore not unreasonable to base the TSH treatment on an effective $\sigma\delta^2$-shell. From Table II such a valence shell is seen to contain 6 bonding or non-bonding orbitals, $S^{\sigma}(a_1)D^{\delta}(t_2)D^{\delta}\bar{D}^{\delta}(e)$, and 6 antibonding orbitals, $\bar{D}^{\delta}(t_1)$ and $P^{\sigma}(t_2)$. In a Co_4^{12+}-moiety, containing 12 electron pairs, all these levels are of course occupied, so that direct metal–metal bonding is excluded: the cluster is held together only by the sulfide bridges. As demonstrated by Simon and Dahl [24] in the singly-oxidized species, the Co–Co distances are indeed shortened, due to the introduction of a hole in an antibonding orbital of t_1 or t_2 symmetry. Moreover the oxidized form is Jahn-Teller distorted, also in agreement with the predicted triply-degenerate nature of the HOMO of the parent compound [24]. According to the present TSH analysis a $P^{\sigma}(t_2)$ assignment of this HOMO is the more likely.

Removal of all twelve antibonding electrons is achieved in the isostructural compound $Cr_4Cp_4(\mu_3\text{-}O)_4$ [25]. In all current electron-counting schemes such a compound would be expected to be a saturated closed-shell T_d cluster, with the same set of inaccessible orbitals as $B_4H_4^{4-}$. However as demonstrated by Bottomley and co-workers [25] this compound has only D_2-symmetry and shows antiferromagnetism. The present TSH treatment sheds some light on these observations in that the LUMO is predicted to be approximately $\bar{D}_d^{\delta}(t_1)$ in character, rather than $\bar{P}_p^{\pi}(t_1)$ as in the tetrahedral boron compound. Tangential d orbitals of the δ-type do not have efficient overlap so that the HOMO–LUMO gap in the hypothetical $T_d\text{-}Cr_4Cp_4O_4$ would be

small. This may account for the antiferromagnetism and the observed distortion. It should be noted though that Extended Hückel Calculations by Bottomley and Grein suggest that the order of the cluster valence orbitals is strongly affected by ligand contributions [26].

(d) Octahedral Clusters with Four Effective Valence Orbitals

A particularly clear example of the use of TSH theory in the construction of cluster bonding patterns is offered by the halide and sulfide clusters of niobium, tantalum, molybdenum and tungsten in their lower oxidation states. The ions $Mo_6Cl_8^{4+}$ and $Mo_6S_8^{4-}$ consist of octahedra of metal atoms with μ_3-bridging ligands over the 8 octahedral faces (**9**). Each Mo atom therefore shows a square-planar coordination. Frequently the six metal atoms are also coordinated to six terminal ligands which extend radially outwards from the apices of the octahedron [27]. In fact this tendency of the square planar sites to become pentacoordinated square pyramidal is at the origin of crystal packing in Chevrel phases [28]. Ions such as $Nb_6Cl_{12}^{2+}$ and $Ta_6Cl_{12}^{2+}$ have twelve μ_2-bridging halides, located over the centres of the twelve octahedral edges (**10**). Again 6 more

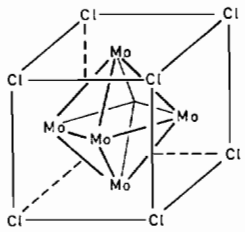

9

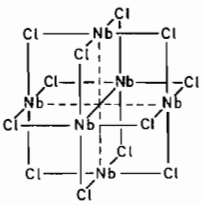

10

exo-ligands may coordinate, giving rise to square pyramidal fragments [27]. In a skeleton-fixed local coordinate frame the Mo-fragments (**11**) appear to be rotated through 45° relative to the Nb-fragments (**12**). As in $Re_3Cl_{12}^{3-}$ (**1**, **2**) the square pyramidal coordination of the fragments requires five hybrids (*e.g.* sp^3d), leaving four effective cluster valence

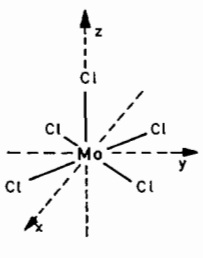

11

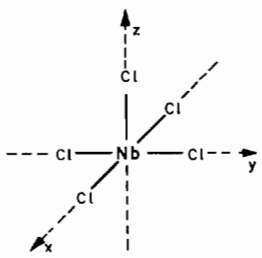

12

orbitals, one σ, two π and one δ. In the Mo-case the δ valence orbital, available for cluster bonding, is $d_{x^2-y^2}$. In the Nb-fragment however one must use the rotamer d_{xy}. These orbitals will be referred to as $\delta(b_1)$ and $\delta(b_2)$ respectively, where the indices are appropriate representational labels of the C_{4v} site-group of the bare sites. (The σ_v-symmetry planes of C_{4v} coincide with the cartesian xy and zy coordinate planes in **11** and **12**). A TSH treatment of these valence orbitals is presented in Table III. We recall that the octahedral symmetry species of the induced molecular orbitals can easily be found, using the method of ascent in symmetry [14, 29]. Symmetry-allowed interactions in the $\sigma\pi^2\delta(b_1)$ and $\sigma\pi^2\delta(b_2)$ bonding patterns will be dealt with separately.

TABLE III. TSH Description of Cluster Molecular Orbitals in an Octahedron. Labels in Brackets Refer to O_h-Representations. The $\delta(b_1)$-based Levels are Needed in Face-bridged Clusters such as $Mo_6Cl_8^{4+}$. The $\delta(b_2)$-based Levels appear in Edge-bridged Clusters, such as $Nb_6Cl_{12}^{2+}$.

	σ	π^2	$\delta(b_1)$ $[Mo_6Cl_8^{4+}]$	$\delta(b_2)$ $[Nb_6Cl_{12}^{2+}]$
bonding	$S^\sigma(a_{1g})$	$P^\pi(t_{1u})$ $D^\pi(t_{2g})$	$D^\delta(e_g)$	$D^\delta(t_{2g})$ $F^\delta(a_{2u})$
antibonding	$P^\sigma(t_{1u})$ $D^\sigma(e_g)$	$\bar{D}^\pi(t_{2u})$ $\bar{F}^\pi(t_{1g})$	$\bar{F}^\delta(a_{2g})$ $\bar{D}^\delta(t_{2u})$	$\bar{D}^\delta(e_u)$

First consider the case of $Mo_6Cl_8^{4+}$. Three pairs of equisymmetric orbitals occur. The $P^\sigma(t_{1u})$ level, which is only weakly antibonding in the TSH scheme, will become strongly antibonding as a result of interaction with $P^\pi(t_{1u})$ [15]. Similarly the e_g orbitals will repel each other but this will not affect the bonding pattern in Table III. However repulsion between the two antibonding t_{2u}-orbitals produces a new bonding combination with predominant $\bar{D}^\delta(t_{2u})$ signature. As a net result 12 bonding orbitals are obtained, $S^\sigma(a_{1g})$ $P^\pi(t_{1u})$ $D^\pi(t_{2g})$ $D^\delta(e_g)$ $\bar{D}^\delta(t_{2u})$, which are completely filled by the 24 valence electrons of the Mo_6^{12+} moiety. In addition the TSH analysis predicts a $\bar{F}^\delta(a_{2g})$ LUMO orbital, the other $\bar{L}^\delta$-type level, $\bar{D}^\delta(t_{2u})$, being removed from the antibonding manifold due to interaction with $\bar{D}^\pi(t_{2u})$. The conclusions are in complete agreement with previous molecular orbital calculations [28]. Furthermore, since the symmetry species of the twelve bonding orbitals coincide with the representations of twelve edge bonds, the analysis supports the accepted view of metal–metal bonding in these clusters in terms of twelve localized 2-centre bonds [16, 30].

In the edge-bridged case of the niobium and tantalum clusters the relevant cluster orbitals derive

from $\sigma\pi^2\delta(b_2)$ fragment orbitals. In this set the t_{1u} and t_{2g} representations occur twice. The interference between the two bonding levels $D^{\pi}(t_{2g})$ and $D^{\delta}(t_{2g})$ is of special importance, since a new antibonding level will result, of predominant δ character. In consequence there are only eight bonding orbitals left, $S^{\sigma}(a_{1g})$ $P^{\pi}(t_{1u})$ $D^{\pi}(t_{2g})$ $F^{\delta}(a_{2u})$, capable of containing exactly 16 electrons, the number available in Nb_6^{14+}. The HOMO is bound to be a pure $F^{\delta}(a_{2u})$ level, which may easily lose two electrons to yield the diamagnetic compound $Nb_6Cl_{12}^{4+}$. Again these conclusions support the qualitative bonding picture of these clusters, as being held together by eight 3-centre face bonds of a_{1g}, t_{1u}, t_{2g} and a_{2u} symmetry [16, 30].

From the point of view of Tensor Surface Harmonic Theory, the Mo–Nb pair is particularly interesting since it is a concrete example of the Stone parity transformation, P, between second rank tensor surface harmonics. P is defined as a simultaneous rotation of each fragment δ-orbital through 45° about the radius vector of the metal atom [14, 31]. It transforms the (unnormalized) tensor surface harmonics in the following way:

$$P L^{\delta} = \bar{L}^{\delta}$$

$$P \bar{L}^{\delta} = -L^{\delta} \qquad (2)$$

At the same time P bridges the angular shift between the Mo and Nb fragments (**11**, **12**) so that the L^{δ} orbitals of the $Mo_6Cl_8^{4+}$ cluster are transformed into the $\bar{L}^{\delta}$ orbitals of the $Nb_6Cl_{12}^{2+}$ cluster and vice versa. Moreover since the parity transformation reverses the bonding or antibonding of a tangential cluster orbital, P relates the HOMO's of the Mo-cluster with the LUMO's of the Nb-cluster and vice versa [32] as shown below (**13**). It is remarkable to note that these conclusions are not affected by

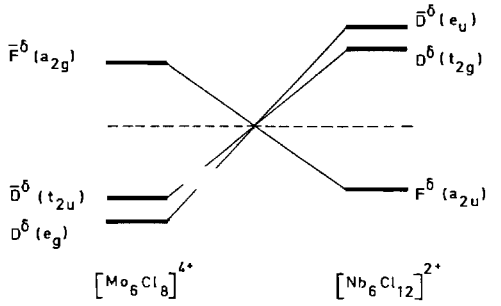

13

orbital interactions with π-orbitals: $\bar{D}^{\delta}(t_{2u})$ is turned into a bonding combination by interaction with $\bar{P}^{\pi}(t_{2u})$, but its parity transform $D^{\delta}(t_{2g})$ is simultaneously turned into an antibonding combination through interaction with $P^{\pi}(t_{2g})$.

Table III also offers a qualitative understanding of the bonding pattern in the electron rich $Co_6(CO)_{14}^{4-}$ metal carbonyl, which has the same face-centered structure as the Mo-compound [33] (**14**). In this case however the bridging ligands cannot be allocated to isolated fragments since CO can only contribute a single electron pair (**15**). Following our

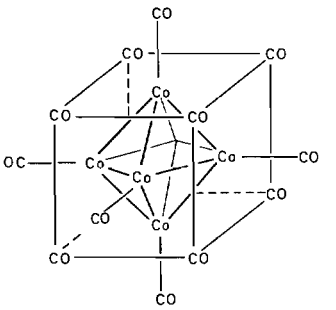

14 **15**

general method only one σ-type valence orbital can therefore be removed for metal–*exo*-ligand coordination, leaving not less than eight effective cluster orbitals, one edge-oriented set $\sigma\pi^2\delta(b_1)$ and one face-oriented set $\sigma\pi^2\delta(b_2)$. A particularly transparent understanding of the bonding can be reached if both sets are treated separately. The eight σ-lone pairs of the bridging CO's will precisely match the eight face-bonding orbitals present in the $\sigma\pi^2\delta(b_2)$ set. Face-coordination of CO therefore raises these metal orbitals above the Fermi level. On the other hand the 16 π-acceptor orbitals of μ_3-CO's transform exactly as the 16 face-antibonding metal orbitals of the same $\sigma\pi^2\delta(b_2)$ set. Interaction will stabilize these orbitals into the bonding region, thereby using 16 metal electron pairs.

As argued by Braterman, coordination of a CO to a triangular metal face therefore follows essentially the same synergic mechanism as the bonding of a terminal CO [34]. In consequence four more valence orbitals per Co atom are completely removed from the effective valence shell, taking with them 32 electrons. The stabilized orbitals will have both metal and ligand π^* character but their detailed composition does not affect the argument. The fragment orbitals, available for cluster bonding, therefore essentially reduce to the $\sigma\pi^2\delta(b_1)$ set, exactly as in the case of the Mo-cluster. The Co_6^{28+} core has two electrons more than Mo_6^{12+}, which will enter the $\bar{F}^{\delta}(a_{2g})$ level. $Co_6(CO)_{14}^{4-}$ and $Mo_6Cl_{14}^{2-}$ are thus essentially iso-electronic, except that as usual all δ-type cluster valence orbitals are filled in the electron rich compound, while in the electron-precise or electron-deficient system the Fermi borderline lies in δ-shell. Extended Hückel Calculations by Mingos on $Co_6(CO)_{14}^{4-}$ confirm the a_{2g} assignment

of the highest occupied bonding or weakly antibonding cluster MO [7].

Even more electrons can be stored in the recently synthesized $Co_6(\mu_3\text{-}S)_8(P(C_2H_5)_3)_6$ cluster [35], which is isostructural to $Mo_6Cl_{14}^{2-}$ and $Co_6(CO)_{14}^{4-}$, but with 14 excess electrons compared to the Mo-cluster, or 12 compared to $Co(CO)_{14}^{4-}$. In this cluster metal–metal distances are considerably lengthened, indicating that the antibonding $\bar{L}^{\pi}$ levels, $\bar{D}^{\pi}(t_{2u})$ and $\bar{P}^{\pi}(t_{1g})$ are also occupied. The remaining inaccessible orbitals are of predominantly $D^{\sigma}(e_g)$ and $P^{\sigma}(t_{1u})$ character.

The analogous $Fe_6(\mu_3\text{-}S)_8(P(C_2H_5)_3)_6^{2+}$ compound [36] has only 6 electrons in excess, as compared to $Mo_6Cl_{14}^{2-}$. Apparently at room temperature all these electrons are unpaired. In the present bonding pattern these electrons must be assigned to 7 possible orbitals of $\bar{F}^{\delta}(a_{2g})$, $\bar{D}^{\pi}(t_{2u})$ and $\bar{P}^{\pi}(t_{1g})$ signature, and predominant d-orbital composition. It is tempting to think that the six electrons will go into the 6 t orbitals but we have no symmetry reason to rule out occupation of a_{2g}. This symmetry assignment is at variance with two conflicting propositions in the literature. In Bacci's United Atom Approach the 7 orbitals transform as the f-orbitals, *i.e.* as $a_{2u} + t_{1u} + t_{2u}$ [37, 38], whereas according to Bottomley and Grein only six orbitals are involved of $a_{1g} + e_g + t_{2u}$ symmetry [26]. In the second case the orbital order is again influenced by metal–ligand interactions.

(e) Octahedral Clusters with Two Effective Valence Orbitals

The $Cp_6Ti_6O_8$ cluster forms a regular octahedral cage, with a diamagnetic ground state [39] (**16**). Each Ti-atom is surrounded by not less than 7 ligand electron pairs, requiring a rather complicated hybrid combination on the metal (**17**).

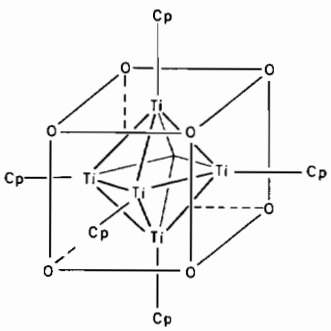

16

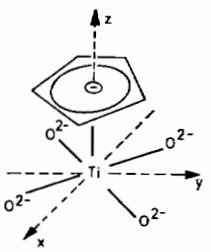

17

In any case only two effective valence orbitals will be available for cluster bonding, one of σ-symmetry and one of δ-symmetry. Using the previous convention the latter orbital may be characterized as $\delta(b_1)$. Clearly such a valence shell will have only one strongly bonding orbital $S^{\sigma}(a_{1g})$, which will accept the two electrons available in a Ti_6^{22+} core. This picture is in agreement with current bonding models [26].

Conclusion

As the numerous applications in the previous section demonstrate, the TSH approach can provide a simple and transparent picture of the bonding in transition-metal clusters. Clearly the treatment suffers from many oversimplifications, which can only be countered in quantitative MO calculations. Even so the crucial orbital characteristics such as the nature of HOMO and LUMO ususally can be predicted correctly from qualitative considerations.

A comparison of bonding patterns in electron-deficient and electron-rich systems clearly illustrates the changing role of the d-orbitals through the transition series. In electron-deficient compounds, from titianium to rhenium, d-orbitals play an important role in the cluster bond formation, while for the electron-rich compounds d-orbitals are usually only weakly interacting and tend to be fully occupied. This change in bonding pattern accompanies the gradual contraction of the d-orbitals through the transition series.

Finally we note that in general the bonding orbitals in clusters do not correlate with the atomic orbitals of an united atom model [37]. As an example a stable compound such as $Co_6(CO)_{14}^{4-}$ with a total of 86 bonding electrons indeed attains the 'magic' number series of the noble gases, but the symmetry of the orbitals involved does not correspond at all with the symmetry of the atomic orbitals of the corresponding pseudo-atom: *e.g.* the 86-electron configuration of $Co_6(CO)_{14}^{4-}$ contains only three a_{1g} orbitals, to be compared with six a_{1g} orbitals in the corresponding radon configuration. Vector and tensor surface harmonics are needed in addition to the ordinary spherical harmonic orbitals of the pseudoatom to give a set of cluster MOs of the correct symmetry [6].

Acknowledgements

P.W.F. would like to thank Prof. L. Vanquickenborne and the Department of Chemistry, KUL, for their hospitality during a visit to Leuven. A.C. is indebted to the British Council for a travel grant under the Guest-Visitor programme and to the Belgian National Science Foundation (NFWO) for a research grant. We thank Dr. Bacci for communicating the results in ref. 38 prior to publication.

References

1 K. Wade, *J. Chem. Soc., Chem. Commun.*, 792 (1971).
2 D. M. P. Mingos, *Nature (London), Phys. Sci., 236*, 99 (1972).
3 R. L. Johnston and D. M. P. Mingos, submitted for publication.
4 A. J. Stone, *Inorg. Chem., 20*, 563 (1981).
5 A. J. Stone, *Polyhedron, 3*, 1299 (1984).
6 A. J. Stone, *Mol. Phys., 41*, 1339 (1980).
7 D. M. P. Mingos, *J. Chem. Soc., Dalton Trans.*, 133 (1974).
8 J. W. Lauher, *J. Am. Chem. Soc., 100*, 5305 (1978).
9 R. G. Woolley, *Nouv. J. de Chim., 5*, 441 (1981).
10 M. Elian and R. Hoffmann, *Inorg. Chem., 14*, 1058 (1975).
11 M. Elian, M. M. L. Chen, D. M. P. Mingos and R. Hoffmann, *Inorg. Chem., 15*, 1148 (1976).
12 R. Hoffmann, *Angew. Chem., Int. Ed. Engl., 21*, 711 (1982).
13 D. G. Evans and D. M. P. Mingos, *Organometallics, 2*, 435 (1983).
14 A. Ceulemans, *Mol. Phys., 54*, 161 (1985).
15 P. W. Fowler and W. W. Porterfield, (1984), to be published.
16 K. Wade, in B. F. G. Johnson (ed.), 'Transition Metal Clusters', Wiley Interscience, Chichester, 1980, p. 193.
17 F. A. Cotton and R. A. Walton, 'Multiple Bonds between Metal Atoms', Wiley Interscience, Chichester, 1982.
18 B. E. Bursten, F. A. Cotton, J. C. Green, E. A. Seddon and G. G. Stanley, *J. Am. Chem. Soc., 102*, 955 (1980).
19 C. Ting-Wah Chu, F. Yip-Kwai Lo and L. F. Dahl, *J. Am. Chem. Soc., 104*, 3409 (1982).
20 C. D. Garner, in B. F. G. Johnson (ed.), 'Transition Metal Clusters', Wiley Interscience, Chichester, 1980, p. 265.
21 R. Saillant, G. Barcelo and H. D. Kaesz, *J. Am. Chem. Soc., 92*, 5739 (1970).
22 R. D. Wilson and R. Bau, *J. Am. Chem. Soc., 98*, 4687 (1976).
23 R. Hoffmann, B. E. R. Schilling, R. Bau, H. D. Kaesz and D. M. P. Mingos, *J. Am. Chem. Soc., 100*, 6088 (1978).
24 G. L. Simon and F. L. Dahl, *J. Am. Chem. Soc., 95*, 2164 (1973).
25 F. Bottomley, D. E. Paez and P. S. White, *J. Am. Chem. Soc., 103*, 5581 (1981).
26 F. Bottomley and F. Grein, *Inorg. Chem., 21*, 4170 (1982).
27 P. R. Raithby, in B. F. G. Johnson (ed.), 'Transition Metal Clusters', Wiley Interscience, Chichester, 1980, p. 1.
28 T. Hughbanks and R. Hoffmann, *J. Am. Chem. Soc., 105*, 1150 (1983).
29 L. L. Boyle, *Acta Crystallogr., Sect. A:, 28*, 172 (1972).
30 S. F. A. Kettle, *Theor. Chim. Acta, 3*, 211 (1965).
31 A. J. Stone and M. J. Alderton, *Inorg. Chem., 21*, 2297 (1982).
32 C. M. Quinn, J. G. McKiernan and D. B. Redmond, *Inorg. Chem., 22*, 2310 (1983).
33 V. G. Albano, P. L. Bellon, P. Chini and V. Scatturin, *J. Organomet. Chem., 16*, 461 (1969).
34 P. S. Braterman, *Struc. Bonding (Berlin), 10*, 57 (1972).
35 F. Cecconi, C. A. Ghilardi, S. Midollini and A. Orlandini, *Inorg. Chim. Acta, 76*, L183 (1983).
36 F. Cecconi, C. A. Ghilardi and S. Midollini, *J. Chem. Soc., Chem. Commun.*, 640 (1981).
37 M. Bacci, *Phys. Lett.*, 99A, 230 (1983).
38 A. Agresti, M. Bacci, F. Cecconi, C. A. Ghilardi and S. Midollini, *Inorg. Chem., 24*, 689 (1985).
39 J. C. Huffman, J. G. Stone, W. C. Krusell and K. G. Caulton, *J. Am. Chem. Soc., 99*, 5829 (1977).